Charge Exchange in Atomic and Molecular Collisions

V. Sidis, Orsay

(Laboratoire des Collisions Atomiques et Moléculaires)

Part II — Theoretical Considerations

The most thorough theoretical studies of charge exchange (CE) have essentially (but not exclusively) been devoted to problems where a *single active electron* is shared by two *inert atomic* or *molecular cores*.

There are two elementary ways of vizualising a CE process. The first viewpoint was proposed by Thomas (1927) who made his argument within the framework of classical mechanics. Since capture in a single binary encounter between the projectile $P^{\alpha+}$ and the target electron may not conserve both energy and momentum, Thomas proposed that CE would occur as a two-step phenomenon (Fig. 9): in the first step, the energetic projectile $P^{\alpha+}$ hits the electron that scatters freely towards the target core T^+; in the second step, the electron bounces off the target-core in such a way that its velocity is parallel and almost equal to that of the projectile.

As an alternative to the above *kinematic* description of CE, the second point of view considers an electron moving in the potential wells associated with the projectile and target cores (Fig. 10). As the atoms approach each other and then recede the height and the thickness of the barrier separating the two wells vary. The electron prepared initially in one well (say T) may overcome the barrier or tunnel through it, if a vacant level exists in front; a subtle *dynamical* competition between the collision time and the oscillation period of the electron in the two wells or the typical tunnelling time thereby determines the probability of remaining trapped in the second well (P).

Fig. 10 — Schematic view of the charge exchange process at low energy. An electron belonging initially to well T may tunnel through the barrier or overcome it when P and T approach each other. In the separation stage of the collision, the barrier rises again and the density around P may be trapped depending on the collision velocity.

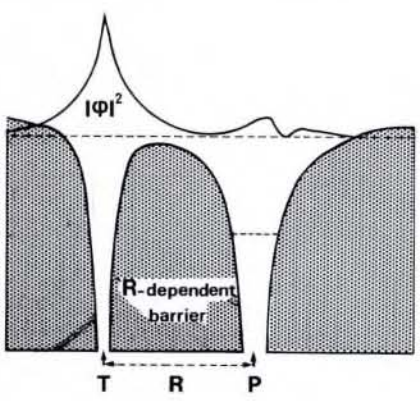

High Energies

The Thomas point of view is likely to apply at high velocities v and rather close encounters so that, in the first step, the electron velocity and its interaction with the target core may be neglected. This model predicts a v^{-11} fall-off of the CE cross-section for $P^{\alpha+}$ + T collisions. Owing to the smallness of total CE cross-sections at high energies (typically $\sigma(\alpha^{-2\,(\text{or}\,-3)}) \lesssim 10^{-19}\text{cm}^2$ for $E \gtrsim 1$ MeV/amu), the corresponding quantum mechanical treatments of CE make use of one form or another of perturbation theory. The simplest treatment of this type is the first Born approximation. Here the CE probability amplitude is essentially determined as the matrix element of the projectile-core potential (*post* form) or that of the target-core (*prior* form) between the relevant unperturbed initial and final states. However, there is a general consent to date to reject this approximation owing not only to its failure to reproduce the experimental data (albeit some improvements may be brought by proper orthogonalisation of the wave functions) but also to its inability to account for the actual v^{-11} behaviour of the CE cross-section at asymptotically high velocities. It is now known that the appropriate description of CE at high energies requires the consideration of terms of order higher than the single electron-projectile or electron-target interaction. It turns out in fact that the second term in the Born series contains the two-step Thomas mechanism where the electron scatters off each core. It is this very term that dominates the high energy behaviour of the *total* cross-section and that determines the behaviour of the *angular differential cross-section* for forward scattering. The prediction by such second order theories that the differential cross-section should display a dip, that reflects an interference between the first and second Born terms, at $\theta_d = 1/2M_P$, followed by a maximum around the Thomas angle $\theta_{Th} = 3^{1/2}/2M_P$ (where M_P is the ratio of the projectile mass to that of the electron), Fig. 11, was nicely confirmed experimentally two years ago.

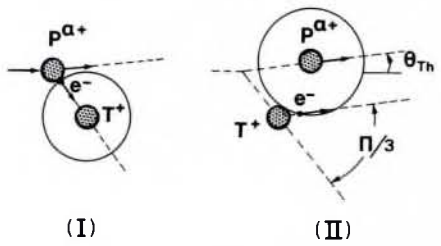

Fig. 9 — The Thomas 2-step (I and II) classical kinematic view of CE. In step I, the active electron, assumed initially at rest in the reference frame of the target, is hit by the projectile and scatters freely towards the target core. In step II, the electron bounces off the target core and emerges with a velocity equal and parallel to that of the projectile. (Θ_{Th} is not to scale).

Another prediction of second order theories is the *electron capture to the continuum* phenomenon. This process is actually viewed as an extension of CE into bound Rydberg states of the projectile, to CE into low energy continuum states beyond the limit of the Rydberg series. The corresponding slow electrons in the projectile reference frame give rise, in the electron energy spectrum measured in the laboratory frame to a cusp shaped structure right around the energy associated with the projectile velocity (Fig. 12). The asymmetry of this peak, also observed experimentally, is another characteristic feature of the second Born theory of CE.

Definitely, there exists a close relation between CE at high energies and ionisa-

Fig. 11 — Comparison of the first (B1) and second (B2) Born CE differential cross-sections for 10 MeV $H^+ + H$ collisions; the characteristic angles Θ_{Th} (Thomas peak) and Θ_D are clearly seen in the B2 result. (Results of Briggs et al. J. Phys. B **17** *(1982) 3085.*

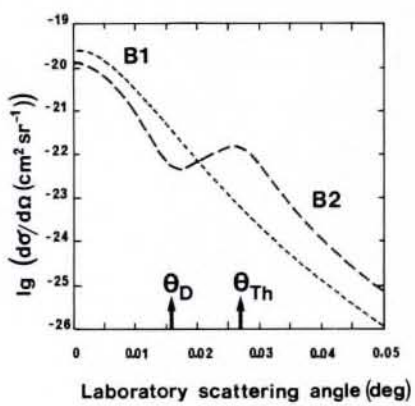

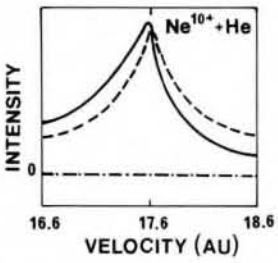

Fig. 12 — Ejected electron velocity spectrum for 17.6 a.u. bare-Ne + He collisions (solid line) illustrating the typical asymmetric cusp shape of the electron capture to the continuum phenomenon; the dashed line, shown for comparison, illustrates how the first Born prediction would look like. (Data from Berry et al. *XIII ICPEAC, Berlin 1983, p. 379).*

tion; this is clearly demonstrated by the process of electron capture from inner-shells of heavy atoms by protons. In such very asymmetric cases it may be shown that the CE probability is approximately given by the ionisation probability of the considered inner-shell multiplied by a probability density factor associated with the bound state of the electron when it is attached to the neutral H product. Consideration of *continuum intermediate states* in the Coulomb field of the P- or T-core characterizes modern treatments which definitely improve upon plane-wave Born approaches. The present theoretical endeavour aims at better taking into account bound intermediate states with a view to improving the quality of the available high energy theories in the intermediate energy regime (10 keV/amu $< E <$ 10 MeV/amu).

Low and Moderate Energies

At low collision energies ($E <$ few keV/amu) the relative P-T velocity ($v <$ 0.1 a.u.) is substantially smaller than typical electron velocities in most bound electronic states ($v_e \cong 1$ a.u.). Accordingly, the collision problem may be viewed as a process of temporary formation and break-up of the quasi-molecule $(PT)^+$; this is the essence of the so-called *quasi-molecular* model of heavy particle collisions. It is within this context that the view of Fig. 10 may be conceived and the corresponding mathematics set up. The great difference between the electronic and nuclear velocities thus enables us to split the treatment of the collision into two parts: (i) a 'static' electronic structure part where the nuclei are regarded as fixed positive charges in the field of which the electrons move, and (ii) a 'dynamic' nuclear part where the nuclei move in the average field of the electrons.

To illustrate the principal ideas of the related theory we shall first take the example of a collision between an atomic ion P^+ and an atom T. According to the above remarks, wave functions

$$\chi_n([\vec{\rho}_i]_{i=1,N}, R)$$

(where $\vec{\rho}_i$ denotes the electron coordinates) are first determined which describe the motion of the N electrons of the system in the two-centre field of the nuclei held fixed at a succession of P-T distances (R). Subsequently, the electron energy levels (V_n) depend parametrically on R. Under certain conditions, it may be shown that $V_n(R)$ are actually the potentials from which derive the forces that act on the nuclei. The determination of the so-called electronic wave functions χ_n and the related potentials V_n is almost routinely done today with the help of computation methods borrowed from the fields of molecular electronic structure and quantum chemistry.

Once the χ_n and V_n are known, one can go one step further and initiate the description of the dynamical evolution of the collision system by letting the nuclei move *'in'* the potentials V_n. It should be kept in mind that the simplest CE (and/or excitation) process ultimately amounts to a change of electronic state ($\chi_{\text{initial}} \rightarrow \chi_n$) of the compound $(PT)^+$ system before it breaks apart. It is thus clear beforehand that the description of the dynamics of CE (and/or excitation) processes will require the treatment of the coupling between the electronic states χ_n induced by the motion of the nuclei. This treatment proceeds as follows; the total wave function of the system that describes both the electrons and the nuclei is expanded as:

$$\Psi([\vec{\rho}_i]_{i=1,N}, \vec{R}) = \Sigma F_n(\vec{R})\, \chi_n([\vec{\rho}_i]_{i=1,N}, \vec{R})$$

and the expansion coefficients F_n called *nuclear functions* are determined, according to the stationary Schrödinger equation, from the set of *close coupling* equations:

$$< \chi_n | H - E | \Psi > = 0 \qquad \forall n$$

or equivalently:

$$(-\tfrac{1}{2}\Delta_R + [V_n(R) - E])\, F_n = \Sigma\, \Omega_{nm} F_m$$

where the r.h.s contains the aforementioned coupling. Obviously, the function $F_n(R)$ contains the information on the probability that the system be in the state χ_n when $R \rightarrow \infty$. Thenceforth, the desired differential and total cross-sections may be derived from the asymptotic behaviour of the nuclear functions.

Owing to the large mass of the projectile and target, the wavelength associated with their relative motion is in many instances short compared to typical ranges of variation of the relevant interactions. Consequently, *semi-classical approximations* may be devised where the nuclear motion is treated classically, and is ascribed a trajectory $\vec{R}$ (t), whereas the electronic motion is still treated quantally. Hence, the CE probability amplitudes may alternatively be determined by solving a time-dependent(-like) Schrödinger equation:

$$(H_{\text{electronic}}([\vec{\rho}_i]_{i=1,N}, \vec{R}(t)) - i\partial/\partial t)\, \Psi([\vec{\rho}_i]_{i=1,N}, \vec{R}(t)) = 0$$

(where $H_{\text{electronic}}$ is the total Hamiltonian H from which the nuclear kinetic energy terms have been removed).

Although several calculations at low energy ($E <$ 100 eV) have been performed within the pure quantum mechanical framework, a majority of works to date have been undertaken using the aforementioned semi-classical treatment not only because it lends itself to transparent interpretations, but also because it enables one to build simplifying models and it provides a natural extension towards high energies.

Large scale calculations based on the above principles are presently feasible and detailed comparisons between theory and experiment are now possible. An outstanding recent achievement that has been made possible by modern computational technology and the advent of array processors is the direct numerical solution of the above time-dependent Schrödinger equation for a few one-electron ion-atom systems and, with the help of some approximations, for some few-electron systems. Such 'exact' computations provide invaluable tests of various stages of theoretical approximations.

Still, our general understanding and conceptual views of CE at low energies stem from simple models. A key concept when one attempts to understand and describe electronic transitions (CE and/

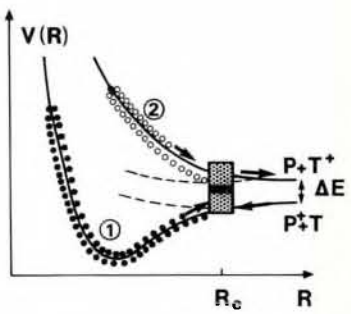

Fig. 13 — Schematic view of the potential energy curves relevant to the discussion of resonant ($\Delta E = 0$) and near-resonant ($\Delta E \neq 0$) CE processes. The dashed lines represent the initially unperturbed energy levels that interact via *the exponential exchange interaction. The arrows and dots indicate the two paths which are involved in the interference that causes oscillations in the differential cross-sections.*

or excitations) at low collision energy is that of *resonance* or *near-resonance*. As a rule of thumb , the closer two electronic energy levels ($V_1(R)$ and $V_2(R)$) lie, the easier a transition may take place between the corresponding states (χ_1 and χ_2). Consider Fig. 13 and let ΔE tend to zero; this situation corresponds to the so-called resonant CE. As the internuclear P - T distance decreases from infinity, the degenerate unperturbed levels (dashed lines) interact via the so-called *exchange interaction* $h(R)$ that behaves typically as $AR^{\upsilon} \exp(-\lambda R)$. This interaction mixes the degenerate states and splits the corresponding unperturbed energy levels thereby giving rise to the potential energy curves $V_{1,2}(R)$. In this simple two-state model the CE probability is found to be a sine function whose argument essentially depends on the area, divided by the collision velocity v, between the curves $V_1(R)$ and $V_2(R)$, from the closest P - T distance of approach to infinity. Qualitatively, this behaviour corresponds indeed to the picture of Fig. 10 where the electron oscillates between the two wells before it remains in one of them as the $(PT)^+$ system breaks apart; at very low velocities an electron may jump back and forth several times whereas at high velocities it may barely achieve a single oscillation. The structures observed in the experimental differential cross-sections for CE in the He^+ He collision, Fig. 5 (*Europhys. News*, April, p. 68), nicely corroborate the above theoretical result. Another simple two-state model is that of near-resonant CE where ΔE is not zero any more but small (few tenths of an eV - few eV). Here, the exchange interaction $h(R)$ mixes efficiently the unperturbed states and splits significantly their energy levels below a critical distance R_c such that: $h(R_c) = \Delta E/2$ (Fig. 13). In this case, the CE probability is a sine function, similar to that discussed for resonant CE, multiplied by the damping factor: $\mathrm{sech}^2(\pi\Delta E/\lambda v_c)$ where v_c is the radial velocity at R_c. It is worth pointing out that this factor involves the competition between two characteristic times: $1/\lambda v_c$ represents a typical collision time whereas $1/\Delta E$ characterizes the time associated with the electron transition. A nice illustration of the behaviour of a differential cross-section for near-resonant CE is given in Fig. 6b (*ibid.* p. 69, full line) for the process:

$$He^+ + Ne \rightarrow He + Ne^+ + 2\ eV$$

The oscillatory behaviour in resonant or non-resonant CE may actually be viewed as an *interference phenomenon* between two waves, Fig. 13: one wave is related to the case when a transition occurs around R_c as P and T approach and no transition occurs as they recede (open circles), whereas the other wave is related to the case when no transition occurs as P and T approach but a transition occurs around R_c as they recede (closed circles). Comparison of the experimental and theoretical patterns provides quite severe tests of the theory.

Integration of the CE probabilities over the impact parameter provides the total cross-section (Fig. 14) which behaves as $(A - B \ln v)^2$ for the resonant case and as $\pi R_c^2 G(2\lambda v/\pi\Delta E)$ in the near-resonant case (G being a universal function). As an illustration, Fig. 1b (*ibid.* p. 66) shows the power of such simple models in their ability to reproduce a wide variety of experimental data for collision systems which may appear awfully complicated at first sight.

We may just mention in passing the phenomenon of *Langevin orbiting* often referred to in the study of collisions at thermal and subthermal energies between ions and non-polar molecules having a dipole polarisability α'. For collisions at very low energy, when the impact parameter b becomes smaller than the radius of the so-called Langevin orbit b_L, where the attractive polarisation potential $(-\alpha'/2R^4)$ starts to prevail over the repulsive centrifugal energy term

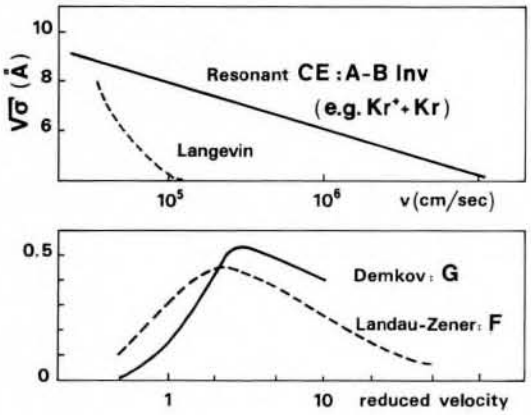

Fig. 14 — Typical shapes of CE cross-sections discussed in text. The reduced velocities for G (the universal function of the Demkov model for near-resonant CE) and for F (the universal function for the Landau-Zener linear curve-crossing model) are respectively $2\lambda v/\pi\Delta E$ and v/γ.

(Eb_L^2/R^2), the collision partners may ideally approach at arbitrary close distances and may thereby reach regions where the electron capture process occurs with a high probability. Hence, CE cross-sections at very low energy are traditionally thought not to exceed the Langevin cross-section (Fig. 14): $\pi b_L^2 = \pi(2\alpha'/E)^{1/2}$. Usually, comparison between an actual experimental cross-section and the Langevin cross-section provides a useful estimate of the efficiency of an investigated CE process. A slightly more complicated expression of the cross-section also exists for the case of ion-polar molecule interactions that are of current interest for the ion-chemistry of interstellar media.

The next question then is: how does CE occur when ΔE is not small any more (several eV)? The alternative mechanism in this case is provided by *crossing of potential energy curves*. Typical examples of this mechanism are found in multiply charged ion + neutral collisions or in ion + ion collisions ($P^{\alpha+}$ + $T^{\beta+}$). In these cases (see *e.g.* Fig. 15) the energy difference between the unperturbed initial and final states varies at large R as:

$\Delta V(R) = |\Delta E| - |(\alpha - 1)(\beta + 1)|/R$ ($\alpha > 1, \beta \geq 0$ or $\alpha = 0, \beta = 0$), owing to the ion-ion Coulomb repulsion (or attraction) in the reactant or product channels or both. Here the exchange interaction $h(R)$ plays a role especially in the vicinity of the curve-crossing $\Delta V(R_x) = 0$. Hence, an acceptable description of this case is provided by a linear curve-crossing model with $\Delta V(R) \cong \xi(R - R_x)$. The corresponding transition probability appears as a sine function times a form factor, depending on the characteristics of the crossing region. Here again the argument of the sine is essentially related to the area, divided by v, between the relevant potentials, from the distance of closest approach to R_x. As already explained above, such an oscillatory behaviour reflects an interference phenomenon between the waves which follow the two paths that are available to the system for $R \leq R_x$ (Fig. 15). The total cross-section entailed by this model is: $\pi R_x^2 F(\gamma/v)$, where F is a universal function (Fig. 14) and $\gamma = 2\pi h^2(R_x)/v\xi$, a parameter characteristic of the crossing zone. Referring again to Fig. 15, it is seen that in $P^{\alpha+}$ + T collision systems with high values of α, curve-crossing mechanisms are likely to provide large cross-sections ($\cong 10^{-14}$ cm^2) for electron capture into highly excited states which subsequently de-excite by hard UV or X-ray emission.

The afore-mentioned mechanisms often occur at large P-T distances of closest approach thereby conveying large cross-sections ($\cong 10^{-14} - 10^{-15}$ cm^2) owing to the geometrical factor $\pi R_{x,c}^2$. Likewise, there are many other mechanisms at moderate ($\cong$ 1Å) and small ($\leq$ 0.5 Å) distances of approach that have been treated successfully within the quasi-molecular model. As a particular example, which also lends itself to a curve-crossing type treatment, is the so-called *diabatic II* process schematized in Fig. 16, where the $e^- - e^-$ repulsion in a doubly occupied molecular orbital (a^2) induces a 2-electron rearrangement process ($a^2 \rightarrow bc$) that entails the reaction: $P^+ + T \rightarrow P + T^{+*}$ or $(P^{-*} + T^+)$. A mechanism of this type is responsible for the CE-excitation process of Fig. 6b (dashed line):

$He^+ + Ne \rightarrow He^*$ (1s, 2l) + Ne^+

Still another mechanism is that schematized in Fig. 17: a transition may occur at very small distances of closest approach where the internuclear axis rotates so suddenly that the electron motion may no longer adjust to that of the nuclei.

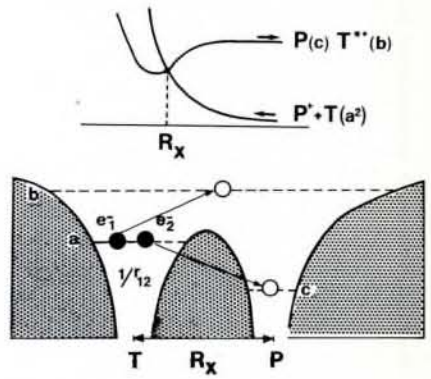

Fig. 16 — Illustration of the so-called Diabatic II mechanism for CE-excitation. Near the curve-crossing of potential energy curves R_x, where the independent-electron energies are such: $2\varepsilon_a \cong \varepsilon_b + \varepsilon_c$, a correlated 2-electron transition from the doubly occupied orbital (a) may occur: one electron fills the inner vacancy (c) while the other electron fills the outer vacancy (b). When T and P recede, the electron in level b may stay around centre T (see e.g. *Fig. 9) thereby producing $P + T^{+*}$.*

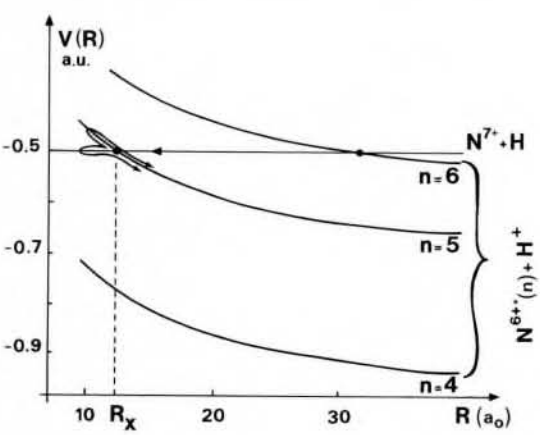

Fig. 15 — Example of a curve crossing pattern involved in CE between a multiply charged ion N^{7+} and a neutral atom H. The two paths involved in the population of the N^{6+*} $(n=5)$ + H^+ channel are shown by arrows. Note the large value of the curve-crossing distances and the actual values of n.

Of course, CE may result from a combination of the above mechanisms *e.g.*: a primary excitation of the $(PT)^+$ quasi-molecule at small distance of approach followed by a near-resonant electron transfer at large R (or *vice versa*). Presently, a qualitative map providing an overall view of the various paths and mechanisms yielding CE and excitation in a given collision system may be obtained in an extremely easy way using so-called *correlation diagrams* that reveal the essential trends of the relevant potential energy curves $V_n(R)$.

One defect of the above quasi-molecular treatment is precisely its starting point, namely: the *clamped nuclei approximation*. Indeed electronic wave functions that are determined holding the nuclei fixed, cannot represent the

translational motion of the electrons with the particular centre to which they initially or finally belong. This is the essence of the so-called *electron translation factor* (ETF) problem which, although known since the early 50s, has received a great deal of attention recently. The conceptually simplest method to overcome this problem is to use an *atomic expansion basis set* involving atomic orbitals multiplied by *plane-wave ETF* that describe the relevant initial and final conditions, nevertheless the nice molecular view is lost. Alternatively, one may try to patch up the quasi-molecular treatment by using a variationally determined common ETF involving a switching function that adjusts the translation motion of the electron according to its proximity to the projectile or target.

Another sub-field showing increasing activity today is *state-to-state* CE in ion + molecule collisions. At low collision energies ($\lesssim$ few eV) a first problem arises when CE competes with reactive scattering or mediates it *e.g.*:

$$P^+ + AB \rightarrow P + AB^+ \quad \text{CE}$$
$$\rightarrow PA + B^+ \quad \text{reactive CE}$$

Although fragmentary pieces of theoretical information have been reported on this problem, using classical trajectories to describe the heavy particle motion and hopping models to describe the electron-transition at crossing seams, it remains widely open. Let us then restrict the discussion to non-reactive CE. Similarly to the ion-atom case the theoretical treatment proceeds in two steps: (i) determination of the relevant electronic wave functions and related couplings for a wide representative sample of geometries of the overall polyatomic system; and, (ii) solution of a large set of close-coupling equations. It is immediately foreseen that the computation task increases tremendously. In the first step the number of relevant geometries increases as a power of the internal nuclear coordinates and in the second step the nuclear motion now consists of the rotations and vibrations of the molecular partners in addition to their relative motion. Our ability to handle both steps obviously rests upon computational technology and on simplifying assumptions. Reduction of the amount of computation effort in step (i) may be achieved using *pseudo-potential* or *model potential* techniques that specifically focus on the few outer electrons which are likely to play an active role during the collision, the effect of the other electrons being treated as a screening of the nuclei. Alternatively, one may use the so-called *diatomics in molecules* method where the polyatomic properties are determined from known diatomic fragment properties. Next, to illustrate the simplifications that may be done in step (ii), let us take for example an atomic-ion + diatomic-neutral collision. At centre of mass collision energies of a few eV/amu, the typical collision time (10^{-14}s) is in general significantly shorter than a characteristic rotation period of the diatom (10^{-11}s). Consequently, the diatom rotation may be held frozen during the solution of close-coupling equations. Moreover, even at such low energies, the conditions of applicability of the semi-classical approximation are often met; thence, the ion-molecule CE process may be described using the aforementioned time-dependent (-like) Schrödinger equation with the simple replacement $H_{\text{electronic}} \rightarrow H_{\text{vibronic}}$ (where vibronic stands for vibrational + electronic).

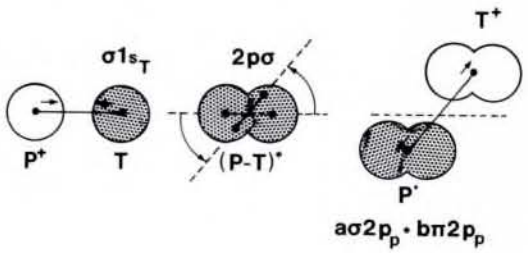

Fig. 17 — Illustration of a rotational coupling mechanism. Left: a $1s_T$ atomic orbital, representing the charge cloud associated with the active electron attached to the target, mixes with a $1s_P$ orbital of the projectile to form an antibonding $2p\sigma$ molecular orbital with a cylindrical symmetry. Middle: the internuclear axis rotates so suddenly that the electron cloud may not follow; the molecular orbital becomes a mixture of $2p\sigma$ and $2p\pi$ orbitals (loss of the initial cylindrical symmetry of the orbital). Right: dissociation of the thus formed electron cloud. The probability that the electron remains around P determines the CE-excitation process.

Attempts at modelling the ion-molecule CE dynamics rest upon the possibility of selecting *two* strongly interacting states in the vibronic network or to represent the problem as a succession of independent 2×2 problems. Active work is currently undertaken in this direction and for about two years a few state-to-state CE processes have been successfully interpreted using adaptations of the simple models discussed above for the ion-atom case. No doubt that the continuous dialogue between experiment, large scale close-coupling calculations and simple models will in the near future provide a detailed understanding of the role of the diatom vibration (and/or rotation) on ion-molecule CE at low energies.

As a conclusion, it is hoped that the present overview has acquainted the reader with: what is charge exchange, how and in which conditions it manifests iself, what are the current experimental and theoretical methods to study it and which physical phenomena it has revealed so far.